

# Orthogonal Convolutional Neural Networks

Jiayun Wang, Yubei Chen, Rudrasish Chakraborty, and Stella X. Yu

Univerisy of California, Berkeley

{peterwg, yubeic, rudra, stellayu}@berkeley.edu

## Abstract

The instability and feature redundancy in CNNs hinders further performance improvement. Using orthogonality as a regularizer has shown success in alleviating these issues. Previous works however only considered the kernel orthogonality in the convolution layers of CNNs, which is a necessary but not sufficient condition for orthogonal convolutions in general.

We propose orthogonal convolutions as regularizations in CNNs and benchmark its effect on various tasks. We observe up to 3% gain for CIFAR100 and up to 1% gain for ImageNet classification. Our experiments also demonstrate improved performance on image retrieval, inpainting and generation, which suggests orthogonal convolution improves the feature expressiveness. Empirically, we show that the uniform spectrum and reduced feature redundancy may account for the gain in performance and robustness under adversarial attacks.

## 1. Introduction

Despite the great success achieved by convolutional neural networks (CNNs) [33, 14, 46], it's widely known that deep neural networks are over-parameterized and their capacities have not been fully utilized in general [1, 12]. Additionally, the training of deep CNNs involves many potential difficulties including exploding/vanishing gradients [8, 17], growth in saddle points [13], feature statistics shifts [29], etc. We observe that a typical convolution layer in CNN viewed as a linear operator has very non-uniform spectrum (Fig.2(b)), which may contribute to the unstable training and exploding/vanishing gradients issues. Furthermore, features learned in deeper layers are highly correlated (Fig.2(a)), which means learned features have high redundancy.

Based on the above observations, we utilize the orthogonality to regularize linear convolutional layers in CNNs to alleviate these issues. Our empirical results demonstrate that orthogonal convolutions encourage more uniform spectrum (Fig.2(b)) and more diverse features (Fig.2(c)) for net-

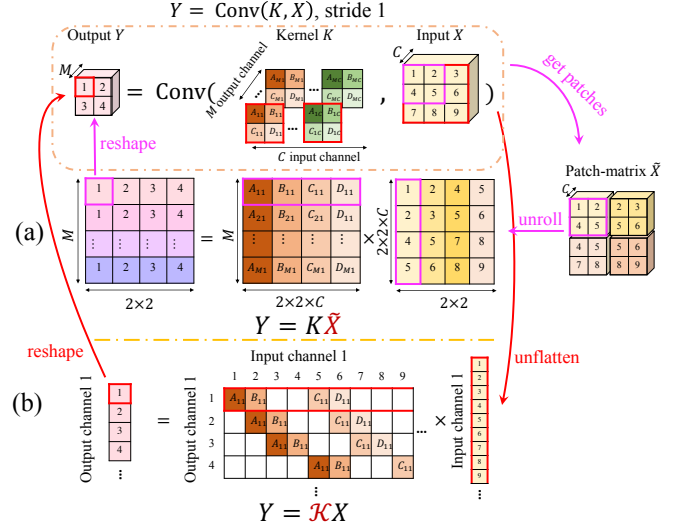


Figure 1. Overview of our approach: A convolution  $Y = \text{Conv}(K, X)$  can be considered as matrix multiplications in two formats: (a) *im2col* methods [53, 25] convert input  $X$  to patch-matrix  $\tilde{X}$  and retain kernel  $K$ ; (b) We convert  $K$  to a doubly block-Toeplitz matrix  $K$  and retain input  $X$ . Our form can be more efficient to analyze the transformation between the input and the output. We further propose efficient algorithm to regularize  $K$  to be orthogonal and observe improved feature expressiveness, task performance and uniform  $K$  spectrum. (Fig.2).

works. As a result, our proposed regularizer leads to superior performances (Fig.2(d)) in many different high-level and low-level vision tasks. Specifically, orthogonal convolution achieves up to 3% gain on CIFAR100, up to 1% gain on ImageNet classification. Consistent gains (3%) in semi-supervised learning on CIFAR100, 1.3 gain in FID on image generation, 2% improvement in fine-grained CUB bird retrieval and an average 4.3 PSNR increase in unsupervised image inpainting indicate improved generalization abilities of the suggested method.

Many works have proposed to use orthogonal linear operation as a type of regularization in training deep neural networks. [6, 52, 4, 5] has shown orthogonal regularization improves the stability and performance of CNNs since it can preserve energy, make spectrum uniform [56], stabilize the activation distribution in different network layers [42] and

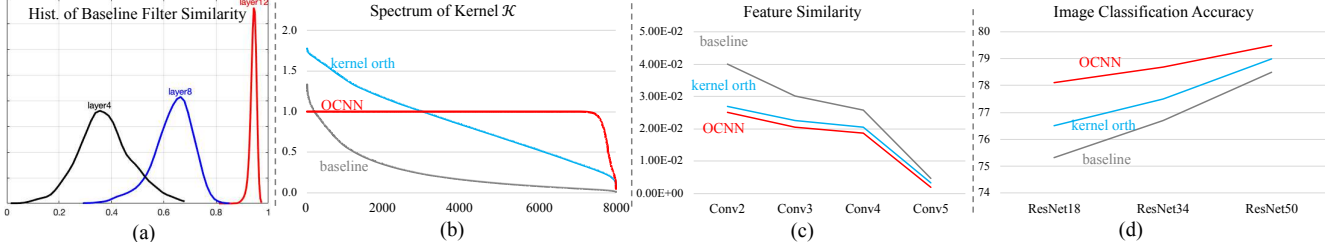


Figure 2. (a) Histograms of pairwise filter similarities of VGG16 for ImageNet show increasing correlation among filters with depth. The similarity is computed between two filters based on their guided back-propagation patterns on a set of images. As the number of channels increases with depth from 64 to 256, more filters become similar. (b) Without regularization, the spectrum of a convolution layer shows large variation. Kernel orthogonality alleviate the issue but still insufficient. OCNNs enforces a uniform spectrum. (c) Feature similarity across channels is reduced. (d) Image classification accuracy on CIFAR100 shows improvement with orthogonal convolution regularization.

remedy the exploding/vanishing gradient issues [2]. In addition, we also show constraining orthogonality among filters for a certain layer leads to smaller correlations among learned features and reduce the filter redundancy, which in return improves the feature expressiveness and task performance.

A convolution layer  $Y = \text{Conv}(K, X)$  can be considered as a linear operation in two different forms (Fig.1): (a) *im2col* methods [53, 25] convert input  $X$  to patch-matrix  $X \mapsto \tilde{X}$  and retain kernel  $K$  as a matrix, i.e.  $Y = K\tilde{X}$ . (b) We convert kernel  $K$  to a doubly block-Toeplitz (DBT) matrix  $\mathcal{K}$  and retain input  $X$ , i.e.  $Y = \mathcal{K}X$ . The second form is more direct to analyze the linear transformation properties between the input  $X$  and the output  $Y$ . Orthogonal regularization can be imposed on either  $K$  or  $\mathcal{K}$ , where we show later in Section 3 the former condition is necessary but not sufficient for the latter one.

Most previous works adopted the *im2col* form and introduce orthogonality to kernel matrix  $K$ , which can be achieved [52, 4, 5] by penalizing the Gram matrix of the kernel to be close to identity matrix  $\|KK^T - I\|$ . More recent works proposed to improve the kernel orthogonality by normalizing spectral norms [37], regularizing mutual coherence [6], and penalizing off-diagonal elements [9]. Despite the improved stability and performance, the orthogonality of  $K$  is insufficient to make a linear convolution layer orthogonal. We show in Fig.2 (b) that the spectrum of  $\mathcal{K}$  still exhibits large variations after  $K$  been made orthogonal.

Our work adopts the Toeplitz matrix format and proposes a better orthogonal convolutional regularization  $\|\text{Conv}(K, K) - I_r\|$  term to CNNs. We call the CNNs with our regularizer *Orthogonal Convolutional Neural Networks* (OCNNs).

In summary, our main contributions are: (a) We propose orthogonal conditions for convolution layers and impose conv-orthogonal regularizers to CNNs. (b) We derive efficient algorithm to implement orthogonal convolutions. (c) We show without additional parameters or much computation overhead, our OCNNs outperform other orthog-

onal regularizers in many different tasks including image classification, generation, retrieval, and inpainting under supervised, semi-supervised and unsupervised settings. The improved feature expressiveness, reduced feature activation correlations, uniform spectrum and enhanced adversarial robustness may account for the performance gain.

## 2. Related Works

We briefly review how *im2col* [53, 25] methods consider convolutions as matrix multiplications, and how kernel orthogonality is constructed. Works related to orthogonal regularizations and training stability are also reviewed.

**Im2col-based Convolutions.** The *im2col* method [53, 25] has been widely used in the current era of deep learning as it enables efficient GPU computation. It transforms the convolution into a GEneral Matrix to Matrix Multiplication (GEMM) problem.

Fig.1 (a) depicts procedures: (a) Given an input  $X$ , we first construct a new input-patch-matrix  $\tilde{X} \in \mathbf{R}^{Ck^2 \times H'W'}$ , by copying patches out of the input and unrolling them into columns of this intermediate matrix. (b) The kernel-patch-matrix  $K \in \mathbf{R}^{M \times Ck^2}$  can then be constructed by reshaping the original kernel weight tensor. Here we use the same notation for simplicity. (c) We can calculate the output

$$Y = K\tilde{X} \quad (1)$$

where we can reshape  $Y$  back to tensor of size  $M \times H \times W$ . This is our desired output of the convolution.

The kernel orthogonal regularization can be defined based on the *im2col* format. The regularizer penalizes the kernel  $K \in \mathbf{R}^{M \times Ck^2}$  to be orthogonal. Specifically, if  $M \leq Ck^2$ , row orthogonal regularizer is

$$L_{\text{korth-row}} = \|KK^T - I\|_F \quad (2)$$

where  $I$  is the identity matrix. Otherwise, column orthogonal may be achieved by

$$L_{\text{korth-col}} = \|K^TK - I\|_F \quad (3)$$

**Kernel Orthogonality in Neural Networks.** Orthogonal kernel have been shown to help alleviate gradient vanishing/exploding problems in recurrent neural networks (RNNs) [15, 51, 34, 2, 49, 41]. Vorontsov [49] discussed the effect of soft versus hard orthogonal constraints on the performances of RNNs. Lezcano-Casado and Martínez-Rubio [34] further proposed a cheap orthogonal constraint based on a parameterization from exponential map.

Orthogonal kernels are also shown to possess the ability to stabilize the training of CNNs [42] and make more efficient optimization [6]. Saxe et al. [44] and [36] proposed to have orthogonal weight for network initialization. The orthogonal initialization utilized the norm-preserving property of orthogonal matrix, which is similar to the effect of batch normalization [29]. However, the kernel orthogonality may not sustain as the training proceeds [44]. Some researchers [21, 39, 28] ensured the orthogonal weight through the whole training by utilizing Stiefel manifold-based optimization methods. Ozay et al. [39] further extended the optimization to convolutional layers and require filters within the same channel to be orthogonal, and observed improved performance. One issue is that weights in CNNs are usually rectangular rather than square matrices. Huang et al. [28] generalized Stiefel manifold property and formulated an Optimization over Multiple Dependent Stiefel Manifolds (OMDSM) problem to overcome this problem. These methods asks the weight to be exact orthogonal and may not be easy to implement and computational cheap in deep CNNs as they usually relies on special optimization methods.

Recent work relaxed and extended the exact orthogonal weight in CNNs. Xie et al. [52] presented orthogonal regularization by enforcing the Gram matrix of the weight matrix to be close to identity under Frobenius norm. The “soft” orthogonal regularization is differentiable and have lower computational cost. Bansal [6] et al. further developed orthogonal regularizations by utilizing mutual coherence and restricted isometry property. It is also worth noting that the orthogonal regularization idea help improve the performance of image generation through generative adversarial networks (GANs) [9, 10, 37].

All the works mentioned above adopted *im2col* format in terms of convolutions. Sedghi et al. [45] utilized DBT matrix to analyze singular values of convolutional layers but did not consider orthogonality. Having orthogonal kernel does not necessarily mean the convolution is orthogonal. In the following sections, we will propose our convolutional orthogonal methods and demonstrate the advantages in comparison with kernel orthogonality.

**Feature Redundancy.** CNNs are shown to have significant redundancy between different filters and feature channels [30, 27]. Many works use the redundancy to compress or speed up networks [20, 24, 27]. The imbalanced distribu-

tion of spectrum may contribute to redundancy in CNNs.

There is an increasing popularity in improving the feature diversity to overcome the problem, including multi-attention [55], diversity loss [35], and orthogonality [11]. We adopt an orthogonal regularizer, which penalizes the kernel  $\mathcal{K}$  so that different filters are orthogonal and share minimal similarity. The analysis and empirical experimental results indicate that our model reduces the feature redundancy and improves the feature diversity.

**Other Techniques to Stabilize the Training of Neural Networks.** There is a vast literature on improving the unstable gradient and co-variate shift problems. Glorot et al. [17] and He et al. [22] proposed near constant variances of each layer for initialization. Ioffe et al. [29] proposed batch normalization to penalize each layer’s input to be similar distribution for reducing the internal covariate shift. Salimans et al. [43] further reparameterized the weight vectors in neural networks and decouples the length of those weight vectors from their direction. Ba et al. [3] proposed layer normalization, which computed the mean and variance used for normalization from all of the summed inputs to the neurons. Pascanu et al. [41] proposed a gradient norm clipping strategy to deal with exploding gradients and a soft constraint for the vanishing gradients problem.

### 3. Orthogonal Convolution

As we mentioned earlier, convolution can be viewed as an efficient matrix vector multiplication, where the matrix  $\mathcal{K}$  is generated by a kernel  $K$ . In order to stabilize the spectrum of  $\mathcal{K}$ , we add orthogonal convolutional regularization to CNNs, which is a stronger condition than kernel orthogonality. We first discuss the view of convolution as a matrix vector multiplication in more detail. Then fast algorithms for constraining row and column orthogonality in convolutions are proposed. In this work, we focus our discussion to the 2D convolution case, but the concepts and conditions generalize to higher dimensional cases.

#### 3.1. Convolution as a Matrix Vector Multiplication

For a convolution layer with input tensor  $X \in \mathbf{R}^{C \times H \times W}$  and kernel  $K \in \mathbf{R}^{M \times C \times k \times k}$ , we denote the convolution’s output tensor  $Y = \text{Conv}(K, X)$ , where  $Y \in \mathbf{R}^{M \times H' \times W'}$ . We can further view  $K$  as  $M$  different filters,  $\{K_i \in \mathbf{R}^{C \times k \times k}\}$ . Since convolution is linear, we can rewrite  $\text{Conv}(K, X)$  in a matrix form:

$$Y = \text{Conv}(K, X) \Leftrightarrow \mathbf{y} = \mathcal{K}\mathbf{x} \quad (4)$$

where  $\mathbf{x}$  is  $X$  flattened to a vector, each row of  $\mathcal{K}$  has non-zero entries corresponding to a particular filter  $K_i$  at a particular spatial location. As a result,  $\mathcal{K}$  can be constructed as a doubly block-Toeplitz (DBT) matrix  $\mathcal{K} \in \mathbf{R}^{(MH'W') \times (CHW)}$  from kernel tensor  $K \in \mathbf{R}^{M \times C \times k \times k}$ .

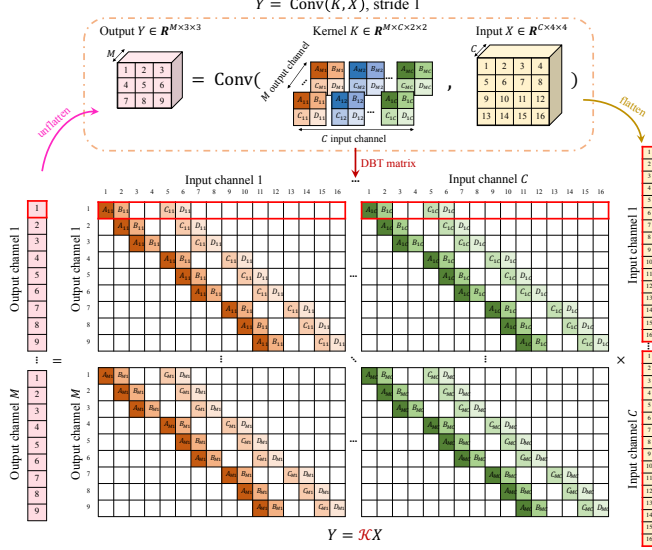


Figure 3. Convolutions based on the doubly block Toeplitz matrix. We first flatten  $X$  to a vector  $\mathbf{x}$ , and then convert weight tensor  $K \in \mathbf{R}^{M \times C \times k \times k}$  as Toeplitz matrix  $\mathcal{K} \in \mathbf{R}^{(MH'W') \times (CHW)}$ . The output  $\mathbf{y} = \mathcal{K}\mathbf{x}$ . We can obtain the desired output  $Y \in \mathbf{R}^{M \times H' \times W'}$  by reshaping  $\mathbf{y}$ . The example has input size  $C \times 4 \times 4$ , kernel size  $M \times C \times 2 \times 2$  and stride 1.

We can obtain the output tensor  $Y \in \mathbf{R}^{M \times H' \times W'}$  by reshaping vector  $\mathbf{y}$  back to the tensor format. Fig.3 depicts an example of convolution with input size  $C \times 4 \times 4$ , kernel size  $M \times C \times 2 \times 2$  and stride 1, based on a DBT matrix.

### 3.2. Convolutional Orthogonality

Depending on the actual configuration of each layer, the corresponding matrix  $\mathcal{K} \in \mathbf{R}^{(MH'W') \times (CHW)}$  may be a fat matrix ( $MH'W' \leq CHW$ ) or a tall matrix ( $MH'W' > CHW$ ). In either case, we would like to regularize the spectrum of  $\mathcal{K}$  to be uniform. In the fat matrix case, the uniform spectrum requires a row orthogonal convolution and the tall matrix case requires a column orthogonal convolution where  $\mathcal{K}$  is a normalized frame [31] and preserves the norm.

In theory, we can implement the doubly block-Toeplitz matrix  $\mathcal{K}$  and enforce the orthogonality condition in a brute force fashion. However, since  $\mathcal{K}$  is highly structured and sparse, much more efficient algorithm exists. In the following, we show equivalent conditions to the row and column orthogonality conditions, which can be easily computed.

**Row Orthogonality.** As we mentioned earlier, each row of  $\mathcal{K}$  corresponds to a filter  $K_i$  at a particular spatial location  $(h', w')$  flattened to a vector, denoted as  $\mathcal{K}(ih'w', \cdot) \in \mathbf{R}^{CHW}$ . The row orthogonality condition is:

$$\langle \mathcal{K}(ih'_1w'_1, \cdot), \mathcal{K}(jh'_2w'_2, \cdot) \rangle = \begin{cases} 1, & (i, h'_1, w'_1) = (j, h'_2, w'_2) \\ 0, & \text{otherwise} \end{cases} \quad (5)$$

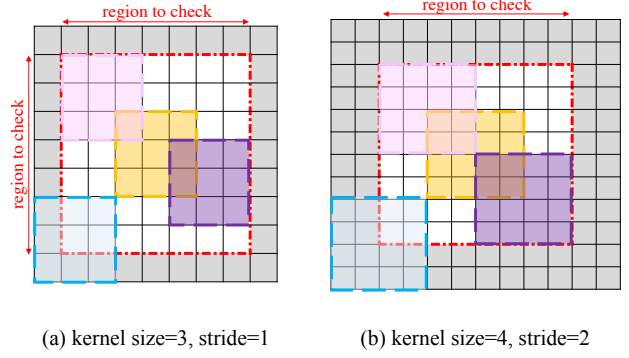


Figure 4. The spatial region to check for row orthogonality. It is only necessary to check overlapping filter patches for the row orthogonality condition. We show two example cases :stride  $S = 1$  with kernel size  $k = 3$  and stride  $S = 2$  with kernel size  $k = 4$ . In both examples, the orange patch is the center patch, and the red border is the region of overlapping patches. For example, pink and purple patches fall into the red region and overlap with the center region; blue patches are not fully inside the red region and they do not overlap with the orange ones. We can use padding to obtain the overlapping regions.

In practice, we do not need to check pairs that the corresponding filter patches do not overlap. It's clear that  $\langle \mathcal{K}(ih'_1w'_1, \cdot), \mathcal{K}(jh'_2w'_2, \cdot) \rangle = 0$  if either  $|h_1 - h_2| \leq k$  or  $|w_1 - w_2| \leq k$  since the two flattened vectors have no support overlap and thus have a zero inner product. So we only need to check the condition where  $|h_1 - h_2|, |w_1 - w_2| < k$ . Due to the spatial symmetry, we can choose fixed  $h_1, w_1$  and only vary  $i, j, h_2, w_2$ , where  $|h_1 - h_2|, |w_1 - w_2| < k$ . Fig.4 shows examples of the region of overlapping filter patches. In general for a convolution, if the kernel size is  $k$  and the stride is  $S$ , the region to check orthogonality can be realized by the original convolution with padding:

$$P = \lfloor \frac{k-1}{S} \rfloor \cdot S. \quad (6)$$

Now we can derive an equivalent condition to Eqn.5 as the following:

$$\text{Conv}(K, K, \text{padding} = P, \text{stride} = S) = I_{r0} \quad (7)$$

where  $I_{r0} \in \mathbf{R}^{M \times M \times (2P/S+1) \times (2P/S+1)}$  has zeros entries except for the center  $M \times M$  entries as an identity matrix. Then minimizing the difference between  $Z = \text{Conv}(K, K, \text{padding} = P, \text{stride} = S)$  and  $I_{r0}$  can give us a near row-orthogonal  $\mathcal{K}$ :

$$\min_K L_{\text{orth}} = \|Z - I_{r0}\|_F^2 \quad (8)$$

**Column Orthogonality.** We use tensor  $E_{i,h,w} \in \mathbf{R}^{C \times H \times W}$  to denote an input tensor, which has all zero except an 1 entry at  $i^{\text{th}}$  input channel, spatial location  $(h, w)$ .



Let's denote  $\mathbf{e}_{ihw} \in \mathbf{R}^{CHW}$  as the flattened vector of  $E_{i,h,w}$ . We can obtain a column  $\mathcal{K}(\cdot, ihw)$  of  $\mathcal{K}$  by multiply  $\mathcal{K}$  and vector  $\mathbf{e}_{ihw}$ :

$$\mathcal{K}(\cdot, ihw) = \mathcal{K}\mathbf{e}_{ihw} = \text{Conv}(K, E_{i,h,w}) \quad (9)$$

here we slightly abuse the equality notation as the reshaping is easily understood. The column orthogonality condition is:

$$\langle \mathcal{K}(\cdot, ih_1w_1), \mathcal{K}(\cdot, jh_2w_2) \rangle = \begin{cases} 1, (i, h_1, w_1) = (j, h_2, w_2) \\ 0, \text{otherwise} \end{cases} \quad (10)$$

Similar to the row orthogonality case, since the spatial size of  $K$  is only  $k$ , Eqn.10 only needs to be checked in a local region where there is spatial overlap between  $\mathcal{K}(\cdot, ih_1w_1), \mathcal{K}(\cdot, jh_2w_2)$ . For the stride 1 convolution case, a much simpler condition, which is equivalent to Eqn.10, exists:

$$\text{Conv}(K^T, K^T, \text{padding} = k - 1, \text{stride} = 1) = I_{c0} \quad (11)$$

where  $K^T$  is the input-output transposed  $K$ , i.e.  $K^T \in \mathbf{R}^{C \times M \times k \times k}$ .  $I_{c0} \in \mathbf{R}^{C \times C \times (2k-1) \times (2k-1)}$  has zeros entries except for the center  $C \times C$  entries as an identity matrix.

**Comparison to Kernel Orthogonality.** The kernel row- and column-orthogonality condition can be written in the following convolution form respectively:

$$\begin{cases} \text{Conv}(K, K, \text{padding} = 0) = I_{r0} \\ \text{Conv}(K^T, K^T, \text{padding} = 0) = I_{c0} \end{cases} \quad (12)$$

where  $I_{r0} \in \mathbf{R}^{M \times M \times 1 \times 1}$ ,  $I_{c0} \in \mathbf{R}^{C \times C \times 1 \times 1}$  are both identity matrices.

It's obvious that the kernel orthogonality condition is a necessary but not sufficient condition for the orthogonal convolution in general. For the case when convolution stride is  $k$ , they are equivalent.

**Orthogonal Regularization in CNNs.** We will add additional orthogonal regularization loss to the final loss of CNNs, so that the task objective and orthogonality regularization can be simultaneously achieved. Denoting  $\lambda > 0$  as the weight of the orthogonal regularization loss, the final loss is:

$$L = L_{\text{task}} + \lambda L_{\text{orth}} \quad (13)$$

where  $L_{\text{task}}$  is the task loss, e.g. softmax loss in image classification task;  $L_{\text{orth}}$  is the orthogonal regularization loss, e.g. Eqn.9 for row-wise convolutional orthogonality.

## 4. Experiments

We conduct 3 sets of experiments to evaluate our orthogonal regularizer on CNNs. The first set benchmark our approaches on standard image classification dataset CIFAR100 and ImageNet, in comparison with other orthogonal regularizers. We additionally benchmark the performance under semi-supervised settings. The second set focus on evaluating the performance of learned features. In terms of high-level visual feature, we experiment on the fine-grained bird image retrieval. In terms of low-level visual feature, we experiment on unsupervised image inpainting. We also evaluate the comprehensive visual feature quality with image generation tasks. The third set of experiments focus on the robustness of OCNNs under adversarial attack. We conclude the section with analysis of our approach in terms of Topelitz kernel  $\mathcal{K}$  spectrum, feature similarity, hyperparameter tuning and space/ time complexity.

### 4.1. Kernel v.s. Conv-orthogonality

The key novelty of our approach is the orthogonal regularization term on convolution layers. We compare both conv-orthogonality and kernel-orthogonal regularizers on CIFAR-100 [32], a dataset with 50, 000 training and 10, 000 images in 100 classes.

We evaluate the image recognition effectiveness using ResNet [23] and WideResNet [54] as backbone network. We add the kernel-orthogonality and our conv-orthogonality as additional regularization terms, without modifying the network architecture. The number of parameters of the network hence does not change.

**Row Orthogonal Regularizers.** The convolutional layers in ResNet [23] satisfy the row orthogonality conditions. Table 1 shows top-1 classification accuracies on CIFAR100. Our approach achieves 78.1%, 78.7%, and 79.5% image classification accuracies on ResNet18, ResNet34 and ResNet50, respectively. Our OCNN outperforms the baseline by 3%, 2%, and 1% over baseline, as well as 2%, 1%, and 1% over the kernel orthogonal regularization.

**Column Orthogonal Regularizers.** The convolution layers in WideResNet [54] satisfy the row orthogonality conditions. Table 2 reports the performance of column orthogonal regularizers with backbone model of WideResNet28 on CIFAR100. Our OCNNs achieves 3% and 1% gain over baseline and kernel orthogonal regularizers.

Table 1. Top-1 accuracies on CIFAR100. Our OCNN outperforms baselines and SOTA orthogonal regularizations.

	ResNet18	ResNet34	ResNet50
baseline [23]	75.3	76.7	78.5
kernel orthogonality [52]	76.5	77.5	78.8
OCNN (ours)	<b>78.1</b>	<b>78.7</b>	<b>79.5</b>

Table 2. WideResNet [54] performance. We apply column orthogonal regularizations and observe improved performance of OCNNs.

	WideResNet [54]	Kernel orth [52]	OCNN
Acc.	77.0	79.3	<b>80.1</b>

## 4.2. Image Classification

We add conv-orthogonal regularizers to the backbone model ResNet34 on ImageNet ILSVRC [14], and compare our method with some representative orthogonal regularization methods.

**Experimental Settings.** We follow the backbone training and evaluation protocols of ResNet34. In particular, the total epoch of the training is 90. We start the learning rate with 0.1, with decreasing by 0.1 every 30 epochs. The weight  $\lambda$  of the regularization loss is 0.1. The model is trained using SGD with momentum 0.9, and the batch size is 256.

**Comparisons.** We compare our method with other orthogonal regularizations, including hard orthogonality OMDSM [28], kernel orthogonality [52] and spectral restricted isometry property regularization [6].

Table 3 shows the Top-1 and Top-5 accuracies on ImageNet. Without additional modification to the backbone model, our OCNN achieves 25.87% and 7.89% top-1 error. Our method outperforms the plain baseline, as well as other orthogonal regularizations by 1%.

Table 3. Top-1 and Top-5 errors on ImageNet [14] with ResNet34 [23]. Our conv-orthogonal regularization outperforms baselines and SOTA orthogonal regularizations.

	Top-1 error	Top-5 error
ResNet34 (baseline) [23]	26.70	8.58
OMDSM [28]	/	9.68
kernel orthogonality [52]	/	8.43
SRIP [6]	/	8.32
OCNN (ours)	<b>25.87</b>	<b>7.89</b>

## 4.3. Semi-supervised Learning

We now study how the proposed OCNNs can benefit other tasks. A common scenario that can benefit from regularization is the semi-supervised learning: when we have a large amount of data of which only a fraction is labeled.

We randomly choose a subset of CIFAR100 as labeled and treat others as unlabeled. We can add the orthogonal regularization to the backbone model without additional modifications. We evaluate the classification performance on the entire validation set for all different fractions.

We vary the proportion of labeled subset from 10% to 80% of the entire dataset. We compare with kernel-orthogonal regularization and report the results in Table 4. Our OCNN constantly outperforms the baseline by 2% - 3% under different fractions of labelled data.

Table 4. Top-1 accuracies on CIFAR100 with an increasing fraction of labeled data. Our conv-orthogonal regularizations are consistently better.

% of training data	10%	20%	40%	60%	80%	100%
ResNet18 [23]	31.2	47.9	60.9	66.6	69.1	75.3
kernel orthogonality [52]	33.7	50.5	63.0	68.8	70.9	76.5
Conv-orthogonality	<b>34.5</b>	<b>51.0</b>	<b>63.5</b>	<b>69.2</b>	<b>71.5</b>	<b>78.1</b>
Our gain	3.3	3.1	2.6	2.6	2.4	2.8

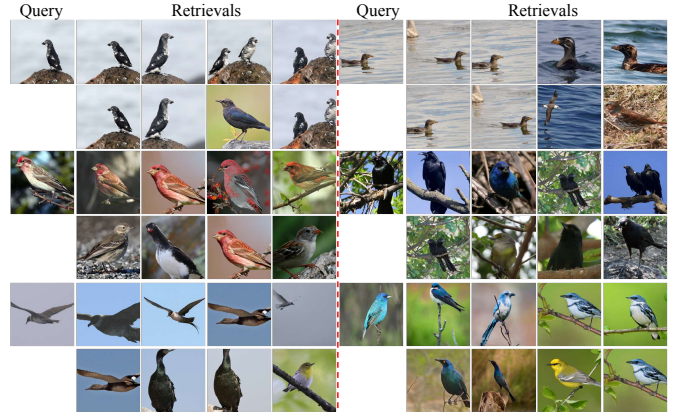


Figure 5. Image retrieval results on CUB-200 Birds Dataset. The model (ResNet34) is trained on ImageNet only. First row shows our OCNN results, while the second row shows the baseline model results. Ours achieves 2% and 3% top-1 and top-5  $k$ -nearest neighbor classification gain.

## 4.4. Fine-grained Image Retrieval

We conduct fine-grained image retrieval experiments on CUB-200 bird dataset [50] to understand the high-level visual feature similarity performance of our conv-orthogonal regularizer. Specifically, we directly use the ResNet34 model trained on ImageNet (from Section ) to obtain the features overall images in the dataset, without further training on the CUB dataset. We observed improved results with our conv-orthogonal regularizer (Fig.5). With conv-orthogonal regularizers, the Top-1  $k$ -nearest-neighbor classification accuracy improves from 25.1% to 27.0%, and Top-5  $k$ -nearest-neighbor classification accuracy improves from 39.4% to 42.3%.

## 4.5. Unsupervised Image Inpainting

To further assess the generalization capacity of the proposed regularization, we add the regularization term to the new task of unsupervised inpainting. In image inpainting, one is given an image  $X_0$  with missing pixels in correspondence of a binary mask  $M \in \{0, 1\}^{C \times H \times W}$  of the same size of the image. The goal is to reconstruct the original image  $X$  by recovering missing pixels:

$$\min E(X; X_0) = \min \|(X - X_0) \odot M\|_F^2 \quad (14)$$

Deep image prior (DIP) [47] proposed to use the prior implicitly captured by the choice of a particular generator

Table 5. Quantitative comparisons on the standard inpainting dataset [26]. Our conv-orthogonality outperforms SOTA methods.

	Barbara	Boat	House	Lena	Peppers	C.man	Couple	Finger	Hill	Man	Montage
Convolutional dictionary learning [40]	28.14	31.44	34.58	35.04	31.11	27.90	31.18	31.34	32.35	31.92	28.05
Deep image prior (DIP) [47]	32.22	33.06	39.16	36.16	33.05	29.8	32.52	32.84	32.77	32.20	34.54
DIP + kernel orthogonality [52]	34.88	34.93	38.53	37.66	34.58	33.18	33.71	34.40	35.98	32.93	36.99
DIP + conv-orthogonality (ours)	<b>38.12</b>	<b>35.15</b>	<b>41.73</b>	<b>39.76</b>	<b>37.75</b>	<b>38.21</b>	<b>35.88</b>	<b>36.87</b>	<b>39.89</b>	<b>33.57</b>	<b>38.48</b>

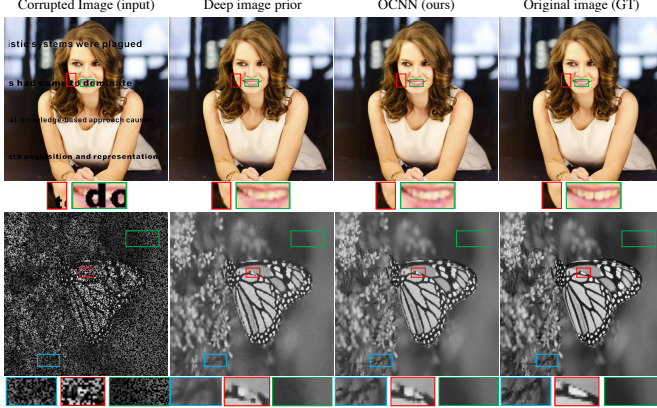


Figure 6. Image inpainting results compared with deep image prior [47]. Top comparison on text inpainting example. Bottom comparison on inpainting 50% of missing pixels. In both cases, our approach outperforms previous methods.

network  $f_\theta$  with parameter  $\theta$ . Specifically, given a code vector/ tensor  $\mathbf{z}$ , they used CNNs as a parameterization  $X = f_\theta(\mathbf{z})$ . The reconstruction goal in Eqn. 14 can be written as:

$$\min_{\theta} \|(f_\theta(\mathbf{z}) - X_0) \odot M\|_F^2 \quad (15)$$

The network can be optimized without training data to recover  $X$ . We further add our conv-orthogonal regularization as an additional prior to the reconstruction goal, to validate if the proposed regularization helps the inpainting:

$$\min_{\theta} \|(f_\theta(\mathbf{z}) - X_0) \odot M\|_F^2 + \lambda L_{\text{orth}}(\theta) \quad (16)$$

In the first example (Fig. 6, top), the inpainting is used to remove text overlaid on an image. Compared with DIP [47], our orthogonal regularization leads to improved reconstruction result of details, especially for the smoothed face outline and finer teeth reconstruction.

The second example (Fig. 6, bottom) considers inpainting with masks randomly sampled according to a binary Bernoulli distribution. Following the procedure in [40, 47], we sample a mask to randomly drop 50% of pixels. For fair comparison, all the methods adopt the same mask. We observe improved background quality, as well as finer reconstruction of the texture of butterfly wings.

We report quantitative PSNR comparisons on the standard data set [25] in Table 5. Our approach outperforms previous state-of-the-art DIP [47] and convolutional sparse

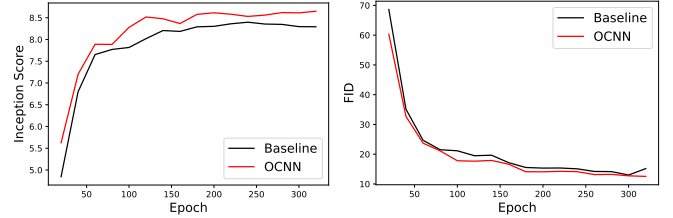


Figure 7. OCNNs have faster convergence for GANs. The IS (left) and FID (right) consistently outperforms the baseline [18] at every epoch.

coding [40]. We also observe gain compared to kernel orthogonal regularizations.

## 4.6. Image Generation

Orthogonal regularizers have shown great success in improving the stability and performance of GANs [10, 37, 9]. We analyze if our convolutional orthogonal regularizer can help train GANs.

We use the best architecture reported in [18], and train for 320 epochs with our convolutional orthogonal regularizer applying on both the generator and discriminator with regularizer weight 0.01, and retain all other settings.

Table 6. Inception Score and Frchet Inception Distance comparison on CIFAR10. Our OCNN outperforms the baseline [18] by 0.3 IS and 1.3 FID.

	IS	FID
PixelCNN [48]	4.60	65.93
PixelIQN [38]	5.29	49.46
EBM [16]	6.78	38.20
SNGAN [37]	8.22	21.70
BigGAN [9]	<b>9.22</b>	14.73
AutoGAN [18]	8.32	13.01
OCNN (ours)	8.63	<b>11.75</b>

The reported model is evaluated 5 times with 50k images each. We achieve  $8.63 \pm 0.007$  inception score (IS) and  $11.75 \pm 0.04$  Frchet inception distance (FID) (Table 6), outperforming the baseline and achieving the state-of-the-art performance. Additionally, we observe faster convergence of GANs with our regularizer (Fig. 7).

## 4.7. Robustness under Attack

The spectrum of  $\mathcal{K}$  is uniform, so each convolution layer approximates 1-Lipschitz function. Given a perturbation

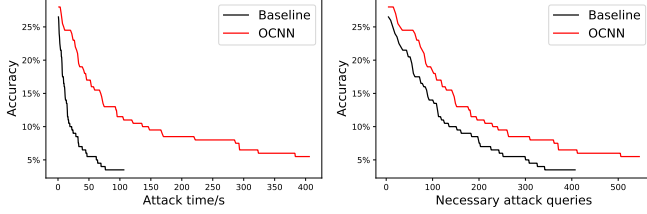


Figure 8. Model accuracy v.s. attack time and necessary attack queries. With our conv-orthogonal regularizer, it takes 7x time and 1.7x necessary attack queries to achieve 90% successful attack rate. Note that baseline ends at accuracy 3.5% while ours ends at 5.5% with the same iteration.

of input  $\Delta x$ , the change of output  $\Delta y$  is bounded to be low. Therefore, the model enjoys robustness under attack because it is hard to search for adversarial examples and the change in output is small and slow.

Table 7. Attack time and number of necessary attack queries needed for 90% successful attack rate.

	Attack time/s	# necessary attack queries
ResNet18 [23]	19.3	27k
OCNN (ours)	136.7	46k

We adopt the simple black box attack [19] to evaluate the robustness of baseline and our OCNN with ResNet18 [23] backbone architecture trained on CIFAR100. The attack basically samples around the input image and finds the “direction” to rapidly decrease the classification confidence of the network by manipulating the input. We only evaluate on the correctly classified test images. The maximum iteration is 10000 with pixel attack. All other settings are retained. We report the attack time and number of necessary attack queries for a specific attack successful rate.

It takes about 7x time and 1.7x attack queries to attack our OCNN, compared with the baseline (Fig.8 and Table 7). Additionally, after the same iterations of the attack, our model has 2% more accuracy than the baseline.

To achieve the same attack rate, baseline models need more necessary attack queries, and searching for such queries is nontrivial and may take time. This may account for the longer attack time of the OCNN.

#### 4.8. Analysis

In order to understand how the conv-orthogonal regularization help improve the performance of CNNs, we analyze several aspects of the proposed method. First, we analyze the spectrum of the DBT matrix  $\mathcal{K}$  to understand how it helps relieve gradient vanishing/exploding. We then analyze the feature similarity after adding the regularization, followed by the influence of the weight  $\lambda$  of the regularization term. Finally, the time and space complexity of OCNNs is analyzed.

**Spectrum of the DBT Kernel Matrix  $\mathcal{K}$ .** For a convolution  $Y = \mathcal{K}X$ , we can analyze the spectrum of  $\mathcal{K}$  to understand

the properties of the convolution. We analyze the spectrum of  $K \in \mathbf{R}^{64 \times 128 \times 3 \times 3}$  of the first convolutional layer of the third convolutional block of ResNet18 network trained on CIFAR100. For fast computation, we use input of size  $64 \times 16 \times 16$ , and solve all the singular values of  $\mathcal{K}$ .

As in Fig.2(b), without regularizations, the spectrum vanishes rapidly, and can cause gradient vanishing problem. Kernel orthogonal regularizations helps the spectrum decrease slower, but still vanishes fast. With our conv-orthogonal regularization, the spectrum almost always stays at 1.0. The uniform spectrum is good at preserving norm and information between convolution layers.

**Feature Similarity.** Orthogonality condition requires the off-diagonal elements to be 0. This means that for every two channels of the output after convolutions, correlations should be relatively small. This can reduce the feature similarity and redundancy across different channels.

We define feature similarity as follows: Given a response map/output tensor  $Y \in \mathbf{R}^{M \times W \times H}$  after a convolutional layer, we can flatten it to matrix  $\tilde{Y} \in \mathbf{R}^{M \times WH}$  by the output channel  $M$ . We can then calculate the correlation matrix over different channels:

$$\text{corr}(\tilde{Y}) = (\text{diag}(K_{YY}))^{-\frac{1}{2}} K_{YY} (\text{diag}(K_{YY}))^{-\frac{1}{2}} \quad (17)$$

where  $K_{YY} = \frac{1}{M}[(Y - \mathbb{E}[Y])(Y - \mathbb{E}[Y])^T]$  is the covariance matrix. If the correlation between any two different channels of features is 0, then the correlation matrix should be identity,  $I \in \mathbf{R}^{M \times M}$ . We can use the distance between the correlation matrix to the identity matrix, normalized by number of off-diagonal items  $M(M - 1)$ , to define feature similarity:

$$\text{feature similarity}(\tilde{Y}) = \frac{\|I - \text{corr}(\tilde{Y})\|}{M(M - 1)} \quad (18)$$

The feature similarity is calculated over the whole test set. We report the feature similarity of different methods in Fig.2(d). When adding kernel orthogonality, the feature similarity decreases across different convolutional blocks. With our convolutional orthogonal regularization, the feature similarity has been further reduced.

**Hyper-parameter Analysis.** We analyze the Influence of the weight  $\lambda$  of the orthogonality loss. As discussed earlier, we achieve the “soft orthogonality” by add additional loss with weight  $\lambda$  to the network. Fig.9 plots the image classification performance of CIFAR100 with backbone model ResNet18 under  $\lambda$  ranging from 0.05 to 1.0. Our approach achieves the best classification accuracy when  $\lambda = 0.1$ .

**Space and Time Complexity.** We analyze the space and time complexity in Table 8. We test the ResNet34 [23] backbone model on ImageNet ILSVRC [14] with a single NVIDIA GeForce GTX 1080 Ti GPU and batchsize 256.

The number of parameters and the test time of the CNN will not change since the regularizer is an additional loss



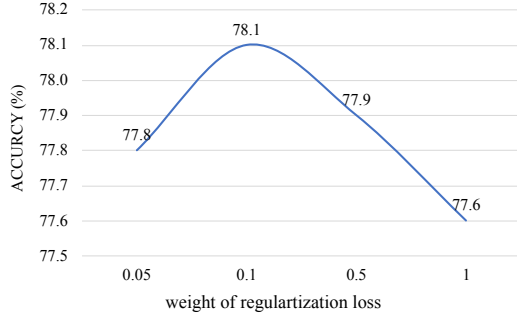


Figure 9. CIFAR100 classification accuracy with different weight  $\lambda$  of the regularization loss. With backbone model ResNet18, we achieve the highest performance at  $\lambda = 0.1$ .

term only during training. With kernel orthogonal regularizers, the training time increase 3%; with conv-orthogonal regularizers, the training time increase 9%.

Table 8. Model size and training/ test time on ImageNet ILSVRC [14].

	ResNet34 [23]	kernel-orth [52]	OCNN
# Params.	21.8M	same	same
Training time (min/epoch)	49.5	51.0	54.1
Test time (min/epoch)	1.5	same	same

## 5. Summary

In this work, we propose efficient algorithms to impose orthogonality condition on convolution layers based on doubly block-Toeplitz matrix, which we call *Orthogonal CNNs*. We show that the kernel orthogonal regularizer adopted by previous works [6, 28] is a necessary but not sufficient condition to orthogonal convolution.

Empirically, we observed OCNNs lead to improved performance on many different tasks including image classification and inpainting under supervised, semi-supervised and unsupervised settings compared to the SOTA orthogonal regularizers. We also show OCNNs help to learn more diverse/expressive visual features with higher training stability, robustness and better generalization.

## References

- [1] Deep compression: Compressing deep neural network with pruning, trained quantization and huffman coding. In *4th International Conference on Learning Representations, ICLR 2016, San Juan, Puerto Rico, May 2-4, 2016, Conference Track Proceedings*, 2016. 1
- [2] M. Arjovsky, A. Shah, and Y. Bengio. Unitary evolution recurrent neural networks. In *International Conference on Machine Learning*, pages 1120–1128, 2016. 2, 3
- [3] J. L. Ba, J. R. Kiros, and G. E. Hinton. Layer normalization. *arXiv preprint arXiv:1607.06450*, 2016. 3
- [4] R. Balestrierio and R. Baraniuk. Mad max: Affine spline insights into deep learning. *arXiv preprint arXiv:1805.06576*, 2018. 1, 2
- [5] R. Balestrierio et al. A spline theory of deep networks. In *International Conference on Machine Learning*, pages 383–392, 2018. 1, 2
- [6] N. Bansal, X. Chen, and Z. Wang. Can we gain more from orthogonality regularizations in training deep cnns? In *Proceedings of the 32nd International Conference on Neural Information Processing Systems*, pages 4266–4276. Curran Associates Inc., 2018. 1, 2, 3, 6, 9
- [7] D. Bau, B. Zhou, A. Khosla, A. Oliva, and A. Torralba. Network dissection: Quantifying interpretability of deep visual representations. In *Proceedings of the IEEE Conference on Computer Vision and Pattern Recognition*, pages 6541–6549, 2017. 12
- [8] Y. Bengio, P. Simard, P. Frasconi, et al. Learning long-term dependencies with gradient descent is difficult. *IEEE transactions on neural networks*, 5(2):157–166, 1994. 1
- [9] A. Brock, J. Donahue, and K. Simonyan. Large scale gan training for high fidelity natural image synthesis. *arXiv preprint arXiv:1809.11096*, 2018. 2, 3, 7
- [10] A. Brock, T. Lim, J. M. Ritchie, and N. Weston. Neural photo editing with introspective adversarial networks. *arXiv preprint arXiv:1609.07093*, 2016. 3, 7
- [11] Y. Chen, X. Jin, J. Feng, and S. Yan. Training group orthogonal neural networks with privileged information. *arXiv preprint arXiv:1701.06772*, 2017. 3
- [12] B. Cheung, A. Terekhov, Y. Chen, P. Agrawal, and B. A. Olshausen. Superposition of many models into one. *CoRR*, abs/1902.05522, 2019. 1
- [13] Y. N. Dauphin, R. Pascanu, C. Gulcehre, K. Cho, S. Ganguli, and Y. Bengio. Identifying and attacking the saddle point problem in high-dimensional non-convex optimization. In *Advances in neural information processing systems*, pages 2933–2941, 2014. 1
- [14] J. Deng, W. Dong, R. Socher, L.-J. Li, K. Li, and L. Fei-Fei. Imagenet: A large-scale hierarchical image database. In *2009 IEEE conference on computer vision and pattern recognition*, pages 248–255. Ieee, 2009. 1, 6, 9, 12
- [15] V. Dorobantu, P. A. Stromhaug, and J. Renteria. Dizzyrnn: Reparameterizing recurrent neural networks for norm-preserving backpropagation. *arXiv preprint arXiv:1612.04035*, 2016. 3
- [16] Y. Du and I. Mordatch. Implicit generation and generalization in energy-based models. *arXiv preprint arXiv:1903.08689*, 2019. 7
- [17] X. Glorot and Y. Bengio. Understanding the difficulty of training deep feedforward neural networks. In *Proceedings of the thirteenth international conference on artificial intelligence and statistics*, pages 249–256, 2010. 1, 3
- [18] X. Gong, S. Chang, Y. Jiang, and Z. Wang. Autogan: Neural architecture search for generative adversarial networks. In *Proceedings of the IEEE International Conference on Computer Vision*, pages 3224–3234, 2019. 7
- [19] C. Guo, J. R. Gardner, Y. You, A. G. Wilson, and K. Q. Weinberger. Simple black-box adversarial attacks, 2019. 8
- [20] S. Han, X. Liu, H. Mao, J. Pu, A. Pedram, M. A. Horowitz, and W. J. Dally. Eie: efficient inference engine on compressed deep neural network. In *2016 ACM/IEEE 43rd*

- Annual International Symposium on Computer Architecture (ISCA)*, pages 243–254. IEEE, 2016. 3
- [21] M. Harandi and B. Fernando. Generalized backpropagation, \‘{E} tude de cas: Orthogonality. *arXiv preprint arXiv:1611.05927*, 2016. 3
- [22] K. He, X. Zhang, S. Ren, and J. Sun. Delving deep into rectifiers: Surpassing human-level performance on imagenet classification. In *Proceedings of the IEEE international conference on computer vision*, pages 1026–1034, 2015. 3
- [23] K. He, X. Zhang, S. Ren, and J. Sun. Deep residual learning for image recognition. In *Proceedings of the IEEE conference on computer vision and pattern recognition*, pages 770–778, 2016. 5, 6, 8, 9, 12
- [24] Y. He, X. Zhang, and J. Sun. Channel pruning for accelerating very deep neural networks. In *Proceedings of the IEEE International Conference on Computer Vision*, pages 1389–1397, 2017. 3
- [25] F. Heide, W. Heidrich, and G. Wetzstein. Fast and flexible convolutional sparse coding. In *Proceedings of the IEEE Conference on Computer Vision and Pattern Recognition*, pages 5135–5143, 2015. 1, 2, 7
- [26] F. Heide, W. Heidrich, and G. Wetzstein. Fast and flexible convolutional sparse coding. In *The IEEE Conference on Computer Vision and Pattern Recognition (CVPR)*, June 2015. 7
- [27] A. G. Howard, M. Zhu, B. Chen, D. Kalenichenko, W. Wang, T. Weyand, M. Andreetto, and H. Adam. Mobilenets: Efficient convolutional neural networks for mobile vision applications. *arXiv preprint arXiv:1704.04861*, 2017. 3
- [28] L. Huang, X. Liu, B. Lang, A. W. Yu, Y. Wang, and B. Li. Orthogonal weight normalization: Solution to optimization over multiple dependent stiefel manifolds in deep neural networks. In *Thirty-Second AAAI Conference on Artificial Intelligence*, 2018. 3, 6, 9
- [29] S. Ioffe and C. Szegedy. Batch normalization: Accelerating deep network training by reducing internal covariate shift. *arXiv preprint arXiv:1502.03167*, 2015. 1, 3
- [30] M. Jaderberg, A. Vedaldi, and A. Zisserman. Speeding up convolutional neural networks with low rank expansions. *arXiv preprint arXiv:1405.3866*, 2014. 3
- [31] J. Kovačević, A. Chebira, et al. An introduction to frames. *Foundations and Trends in Signal Processing*, 2(1):1–94, 2008. 4
- [32] A. Krizhevsky, G. Hinton, et al. Learning multiple layers of features from tiny images. Technical report, Citeseer, 2009. 5
- [33] A. Krizhevsky, I. Sutskever, and G. E. Hinton. Imagenet classification with deep convolutional neural networks. In *Advances in neural information processing systems*, pages 1097–1105, 2012. 1
- [34] M. Lezcano-Casado and D. Martínez-Rubio. Cheap orthogonal constraints in neural networks: A simple parametrization of the orthogonal and unitary group. *arXiv preprint arXiv:1901.08428*, 2019. 3
- [35] S. Li, S. Bak, P. Carr, and X. Wang. Diversity regularized spatiotemporal attention for video-based person re-identification. In *Proceedings of the IEEE Conference on Computer Vision and Pattern Recognition*, pages 369–378, 2018. 3
- [36] D. Mishkin and J. Matas. All you need is a good init. *arXiv preprint arXiv:1511.06422*, 2015. 3
- [37] T. Miyato, T. Kataoka, M. Koyama, and Y. Yoshida. Spectral normalization for generative adversarial networks. *arXiv preprint arXiv:1802.05957*, 2018. 2, 3, 7
- [38] G. Ostrovski, W. Dabney, and R. Munos. Autoregressive quantile networks for generative modeling. In J. Dy and A. Krause, editors, *Proceedings of the 35th International Conference on Machine Learning*, volume 80 of *Proceedings of Machine Learning Research*, pages 3936–3945, Stockholmssan, Stockholm Sweden, 10–15 Jul 2018. PMLR. 7
- [39] M. Ozay and T. Okatani. Optimization on submanifolds of convolution kernels in cnns. *arXiv preprint arXiv:1610.07008*, 2016. 3
- [40] V. Pappayan, Y. Romano, J. Sulam, and M. Elad. Convolutional dictionary learning via local processing. In *The IEEE International Conference on Computer Vision (ICCV)*, Oct 2017. 7
- [41] R. Pascanu, T. Mikolov, and Y. Bengio. On the difficulty of training recurrent neural networks. In *International conference on machine learning*, pages 1310–1318, 2013. 3
- [42] P. Rodríguez, J. Gonzalez, G. Cucurull, J. M. Gonfaus, and X. Roca. Regularizing cnns with locally constrained decorrelations. *arXiv preprint arXiv:1611.01967*, 2016. 1, 3
- [43] T. Salimans and D. P. Kingma. Weight normalization: A simple reparameterization to accelerate training of deep neural networks. In *Advances in Neural Information Processing Systems*, pages 901–909, 2016. 3
- [44] A. M. Saxe, J. L. McClelland, and S. Ganguli. Exact solutions to the nonlinear dynamics of learning in deep linear neural networks. *arXiv preprint arXiv:1312.6120*, 2013. 3
- [45] H. Sedghi, V. Gupta, and P. M. Long. The singular values of convolutional layers. *arXiv preprint arXiv:1805.10408*, 2018. 3
- [46] K. Simonyan and A. Zisserman. Very deep convolutional networks for large-scale image recognition. *arXiv preprint arXiv:1409.1556*, 2014. 1
- [47] D. Ulyanov, A. Vedaldi, and V. Lempitsky. Deep image prior. In *The IEEE Conference on Computer Vision and Pattern Recognition (CVPR)*, June 2018. 6, 7
- [48] A. Van den Oord, N. Kalchbrenner, L. Espeholt, O. Vinyals, A. Graves, et al. Conditional image generation with pixel-cnn decoders. In *Advances in neural information processing systems*, pages 4790–4798, 2016. 7
- [49] E. Vorontsov, C. Trabelsi, S. Kadoury, and C. Pal. On orthogonality and learning recurrent networks with long term dependencies. In *Proceedings of the 34th International Conference on Machine Learning-Volume 70*, pages 3570–3578. JMLR. org, 2017. 3
- [50] P. Welinder, S. Branson, T. Mita, C. Wah, F. Schroff, S. Belongie, and P. Perona. Caltech-UCSD Birds 200. Technical Report CNS-TR-2010-001, California Institute of Technology, 2010. 6

- [51] S. Wisdom, T. Powers, J. Hershey, J. Le Roux, and L. Atlas. Full-capacity unitary recurrent neural networks. In *Advances in Neural Information Processing Systems*, pages 4880–4888, 2016. [3](#)
- [52] D. Xie, J. Xiong, and S. Pu. All you need is beyond a good init: Exploring better solution for training extremely deep convolutional neural networks with orthonormality and modulation. In *Proceedings of the IEEE Conference on Computer Vision and Pattern Recognition*, pages 6176–6185, 2017. [1](#), [2](#), [3](#), [5](#), [6](#), [7](#), [9](#)
- [53] K. Yanai, R. Tanno, and K. Okamoto. Efficient mobile implementation of a cnn-based object recognition system. In *Proceedings of the 24th ACM international conference on Multimedia*, pages 362–366. ACM, 2016. [1](#), [2](#)
- [54] S. Zagoruyko and N. Komodakis. Wide residual networks. *arXiv preprint arXiv:1605.07146*, 2016. [5](#), [6](#)
- [55] H. Zheng, J. Fu, T. Mei, and J. Luo. Learning multi-attention convolutional neural network for fine-grained image recognition. In *Proceedings of the IEEE international conference on computer vision*, pages 5209–5217, 2017. [3](#)
- [56] J. Zhou, M. N. Do, and J. Kovacevic. Special paraunitary matrices, cayley transform, and multidimensional orthogonal filter banks. *IEEE Transactions on Image Processing*, 15(2):511–519, 2006. [1](#)

## Supplementary

The supplementary material provides intuitive explanations of our approach (Section A) and network dissection results to understand the change in feature redundancy/expressiveness (Section B).

### A. Intuitive Explanations of our Approach

We analyze a convolution layer which transforms input  $X$  to output  $Y$  with learnable kernel  $K$ :  $Y = \text{Conv}(K, X)$  in CNNs. Writing in linear matrix multiplication form  $Y = \mathcal{K}X$  (Fig.1(b) of the paper), we simplify the analysis from the perspective of linear systems. We do not use *im2col* form  $Y = K\tilde{X}$  (Fig.1(a) of the paper) as there is an additional structured linear transform from  $X$  to  $\tilde{X}$ , which does not necessarily have a uniform spectrum.

The spectrum of  $\mathcal{K}$  reflects the scaling property of the convolution layer: different input  $X$  (such as cat, dog, and house images) would scale up by  $\eta = \frac{\|Y\|}{\|X\|}$ . The scaling factor  $\eta$  also reflects the gradient scaling. Typical CNNs have very imbalanced convolution spectrum (Fig.2(b) of the paper): for some inputs, it scales up to 2; for others, it scales by 0.1. For a deep network, these irregular spectrums add up and can potentially lead to gradient exploding and vanishing issues.

Features learned by CNNs are also more redundant due to the imbalanced spectrum (Fig.2(a) of the paper). This comes from the diverse learning ability to different images and leads to feature redundancy. A uniform spectrum distribution could alleviate the problem.

To alleviate the problem, we propose to make convolution orthogonal by making  $\mathcal{K}$  orthogonal. Orthogonal convolution regularizer in CNNs (OCNNs) leads to uniform  $\mathcal{K}$  spectrum as expected, and further reduce the feature redundancy and improve the performance (Fig.2(b)(c)(d) of the paper).

Besides classification performance improvements, we also observe improved visual features, both in high-level (image retrieval) and low-level (image inpainting). Our OCNNs also generate realistic images (Section 4.6) and is robust to attacks (Section 4.7).

### B. Network Dissection

We demonstrate in Section 4 that our orthogonal convolutions reduce the feature redundancy by decorrelating different feature channels and enhances the feature expressiveness with improved performance in image retrieval, inpainting and generation. Network dissection [7] is utilized to further evaluate the feature expressiveness across channels.

Network dissection [7] is a framework that quantifies the interpretability of latent representations of CNNs by evaluating the alignment between individual hidden units and a

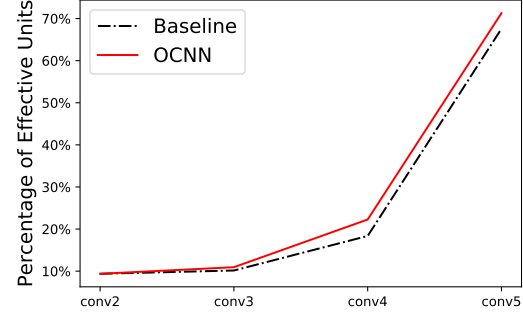


Figure 10. Percentage of effective units ( $\text{mIoU} \geq 0.04$ ) over different layers. Our OCNN has more effective units compared to baseline ResNet34 [23] at each layer.

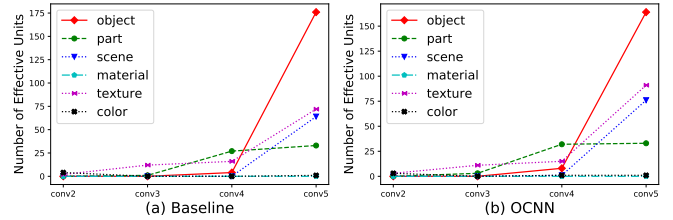


Figure 11. Distribution of concepts of effective units ( $\text{mIoU} \geq 0.04$ ) of different layers. Our OCNN has more uniform concept distribution compared to baseline ResNet34 [23].

set of semantic concepts. Specifically, we evaluate the baseline and our OCNN with backbone architecture ResNet34 [23] trained on ImageNet. The models are evaluated on Broden [7] dataset, where each image was annotated with spatial regions of different concepts, including cat, dog, house, etc. The concepts are further grouped into 6 categories: scene, object, part, material, texture and color. Network dissection framework compares the mean intersection over union ( $\text{mIoU}$ ) between network channel-wise activation of each layer and ground-truth annotations. The units/feature channels are considered as “effective” when  $\text{mIoU} \geq 0.04$ .

Our OCNN (Table 9 and Fig.10) have more effective units over different layers of the network. Additionally, the distribution of 6 concept categories is more uniform for our OCNN (Fig.11). The results imply that orthogonal convolutions reduce feature redundancy and enhance the feature expressiveness.

Table 9. Number of units/feature channels with  $\text{mIoU} \geq 0.04$  comparisons on ImageNet ILSVRC [14].

	conv2	conv3	conv4	conv5
ResNet34 [23]	6	13	47	346
OCNN (ours)	6	14	57	365